

Low temperature hydrothermal and solution synthesis of CeO₂ nanoparticles: A comparative investigation

Shahin Khademinia¹, Mahdi Behzad^{1,*}, Abdolali Alemi², Mahboubeh Dolatyari³,

Murat Sertkul⁴

¹ Department of Chemistry, Semnan University, Semnan 35351-19111, Iran

² Department of Inorganic Chemistry, Faculty of Chemistry, University of Tabriz, Tabriz, Iran

³ Laboratory of Nano Photonics & Nano Crystals, School of Engineering-Emerging Technologies, University of Tabriz, Tabriz, Iran

⁴ Department of Physics Engineering, Istanbul Technical University, Maslak, 34469, TR

Article history:

Received: 31/May/2014

Received in revised form: 11/Jul/2014

Accepted: 26/Jun/2014

Abstract

Nanostructured CeO₂ powders were synthesized via a series of hydrothermal and solution precipitation methods. Three different hydrothermal methods including 1:2 and 1:1 Bi:Ce molar ratios at 180 °C for 48 h (S₁ and S₂, respectively) without calcinations; and 2:1 Bi:Ce molar ratio at 180 °C for 48 h with calcinations (S₃) were performed successfully for the synthesis of the target nanomaterials. Two different solution precipitation methods i.e. 1:1 Bi:Ce molar ratio at 80 °C for 40 min without and with calcinations (S₄ and S₅, respectively) were also used for the synthesis of CeO₂ nanoparticles. Bi(NO₃)₃ and (NH₄)₂Ce(NO₃)₆ were used as raw materials. The synthesized materials were characterized by powder X-ray diffraction (PXRD) technique. CeO₂ crystallized in a cubic crystal structure with cell parameters of a=b=c= 5.412 Å. The morphologies of the synthesized materials were studied by field emission scanning electron microscopy (FESEM). The technique showed that the morphology of the synthesized nanomaterials were strongly dependent on the synthetic procedure.

Keywords: Cerium Oxide, Hydrothermal, Nanomaterials, PXRD.

1. Introduction

Recently, cerium oxide (CeO₂) has been extensively studied for their structural and chemical properties. Ceria (CeO₂) has fluorite type crystal structure with space group

Fm3m. Ceria is an important material in various fields, such as catalysis, microelectronics, optoelectronics, electrochemical devices, ultraviolet blockers, etc. [1–3]. Nanostructured ceria (cerium oxide, CeO₂) with a cubic fluorite structure has been considered as one of the most

* Corresponding Author: EMail: mbehzad@semnan.ac.ir, mahdibehzad@gmail.com, Tel: +98-233 338 3195

reactive rare earth oxides with a wide-energy-gap (5.5 eV) [4]. Many researchers have prepared nanosized CeO_2 particles using several methods such as thermal decomposition [5], hydrothermal synthesis [6], sol-gel processing [7], reverse micelles route [8], sonochemistry [9], microwave-assisted heating routes [10], flame spray pyrolysis [11], homogeneous precipitation with urea or hexamethylenetetramine [12], combustion synthesis [13], solvothermal oxidation [13], surfactant method [14] and so on. Cerium oxide (CeO_2) is commercially an important part of oil-refining catalysts and automotive exhaust gas converters, as an oxidation catalyst for combustion of carbonaceous deposits in diesel exhaust gas particulate traps and as an oxygen and electron-transfer agent in catalysts for the ammoxidation of propylene in the production of acrylonitrile [15]. Also, Ceria (CeO_2) is widely used in solid oxide fuel cells (SOFC), polishing agents and luminous materials [16]. In this work we have investigated the synthesis of CeO_2 nanomaterials by different conditions in hydrothermal method.

2. Experimental

2.1. Materials and methods

All chemicals were of analytical grade, obtained from commercial sources, and used without further purification. Phase identifications were performed on a powder X-ray diffractometer D5000 (Siemens AG, Munich, Germany) using $\text{CuK}\alpha$ radiation. The morphology of the obtained materials was examined with a field emission scanning electron microscope (Hitachi FE-SEM model S-4160).

2.2. Hydrothermal synthesis of CeO_2 nanomaterials

2.2.1. Synthesis procedure of S_1

In a typical synthetic experiment, S_1 was synthesized as follow: 0.49 g (1.0 mmol) of $\text{Bi}(\text{NO}_3)_3 \cdot 5\text{H}_2\text{O}$ ($M_w = 485.07 \text{ gmol}^{-1}$) and 1.10 g (2.0 mmol) of $(\text{NH}_4)_2\text{Ce}(\text{NO}_3)_6 \cdot 6\text{H}_2\text{O}$ ($M_w = 548.32 \text{ gmol}^{-1}$) with Bi:Ce molar ratio of 1:2 were added to 70 mL of hot aqueous solution of 0.5M NaOH under magnetic stirring at 80 °C. The solution was stirred further for 15 min. The resultant solution was transferred

into a 100-mL Teflon lined stainless steel autoclave. The autoclave was sealed and heated at 180 °C for 48 h. When the reaction was completed, it cooled to room temperature by water immediately. Then the prepared powders were washed with distilled water and dried at 120 °C for 20 min under normal atmospheric conditions.

2.2.2. Synthesis procedure of S_2

S_2 was synthesized following similar procedure as described for S_1 , except 1:1 molar ratio Bi:Ce was used: 0.97 g (2.0 mmol) of $\text{Bi}(\text{NO}_3)_3 \cdot 5\text{H}_2\text{O}$ ($M_w = 485.07 \text{ gmol}^{-1}$) and 1.10 g (2.0 mmol) of $(\text{NH}_4)_2\text{Ce}(\text{NO}_3)_6 \cdot 6\text{H}_2\text{O}$ ($M_w = 548.32 \text{ gmol}^{-1}$).

2.2.2. Synthesis procedure of S_3

S_3 was synthesized following similar procedure as described for S_1 , except 2:1 molar ratio Bi:Ce was used: 0.97 g (2.0 mmol) of $\text{Bi}(\text{NO}_3)_3 \cdot 5\text{H}_2\text{O}$ ($M_w = 485.07 \text{ gmol}^{-1}$) 0.55 g (1.0 mmol) of $(\text{NH}_4)_2\text{Ce}(\text{NO}_3)_6 \cdot 6\text{H}_2\text{O}$ ($M_w = 548.32 \text{ gmol}^{-1}$). When the hydrothermal reaction was performed, the collected powders (S_3) were taken for further thermally treatment. S_3 was treated more thermally at 500 °C for 6h. When the reaction completed and allowed to cool slowly to room temperature, a yellowish powder was collected.

2.3. Low temperature solution synthesis of CeO_2 nanomaterials

2.3.1. Synthesis procedure of S_4

In a typical synthetic experiment, 0.97 g (2.0 mmol) of $\text{Bi}(\text{NO}_3)_3 \cdot 5\text{H}_2\text{O}$ ($M_w = 485.07 \text{ gmol}^{-1}$) and 1.10 g (2.0 mmol) of $(\text{NH}_4)_2\text{Ce}(\text{NO}_3)_6 \cdot 6\text{H}_2\text{O}$ ($M_w = 548.32 \text{ gmol}^{-1}$) with Bi:Ce molar ratio of 1:1 were added to 70 mL of deionize water under magnetic stirring at 80 °C for 40 min. After the reaction was performed, the prepared powder washed with distilled water and dried at 120 °C for 20 min under normal atmospheric conditions. In a similar rout, the prepared powders were treated thermally at 500 °C for 6h.

2.3.2. Synthesis procedure of S_5

S_5 was synthesized following similar procedure as described for S_4 , except that calcinations treatment was used: The collected powders were treated thermally at 500 °C for 6h.

3. Results and discussions

Figures 1 and 2 show the PXRD patterns of the synthesized CeO₂ nanomaterials via hydrothermal and low temperature solution methods. Figure 1 shows the PXRD patterns of S₁ to S₃. It was found that the obtained phase is a cubic CeO₂. The data reported in the present study is consistent with Joint Committee for Powder Diffraction Studies (JCPDS) card numbers 34:10,062 and 51:0231. However, it is clear that the peak intensity and the Full width at half maximum (FWHM) of the PXRD patterns of the synthesized nanomaterials are different from each other that will affect on the crystal sizes. The interplanar spacing (*d*) of S₁, S₂ and S₃ were calculated by Bragg's equation using the peak position at miller indices of 111. For example, comparing the data for S₁ and S₃, it was found that there is an expansion in the unit cell: $\Delta 2\theta = \theta(S_3) - \theta(S_1) = 28.00 - 28.24 = -0.24^\circ$. So, $\Delta d = d(S_3) - d(S_1) = 3.183 - 3.156 = 0.027 \text{ \AA}$.

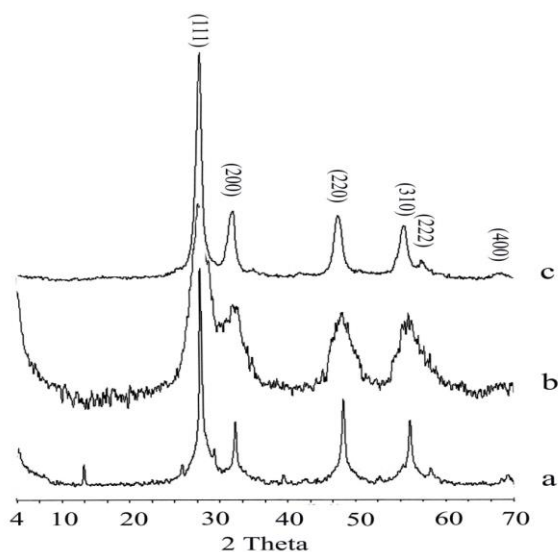


Figure 1: PXRD patterns of a) S₁, b) S₂ and c) S₃.

Figure 2 shows the PXRD patterns of S₄ and S₅. It was found that the main phase is CeO₂ [1-3]. However, the patterns shape and intensity of S₄ and S₅ is different from those of S₁ to S₃. It shows that the crystal planes orientations and their growth in a specific 2 θ are different from each other. So there should be a clear different in interplanar spacing compared to those of S₁ to S₃. The calculated interplanar spacing for S₄ and S₅ using the peak at miller

indices of 111 is as follow: $\Delta 2\theta = \theta(S_5) - \theta(S_4) = 28.12 - 28.94 = -0.82^\circ$. So, $\Delta d = d(S_5) - d(S_4) = 3.17 - 3.08 = 0.09 \text{ \AA}$. So there is an expansion in the unit cell. However, the value of the expansion for S₅ compared to S₄ is higher than that of S₃ compared to S₁.

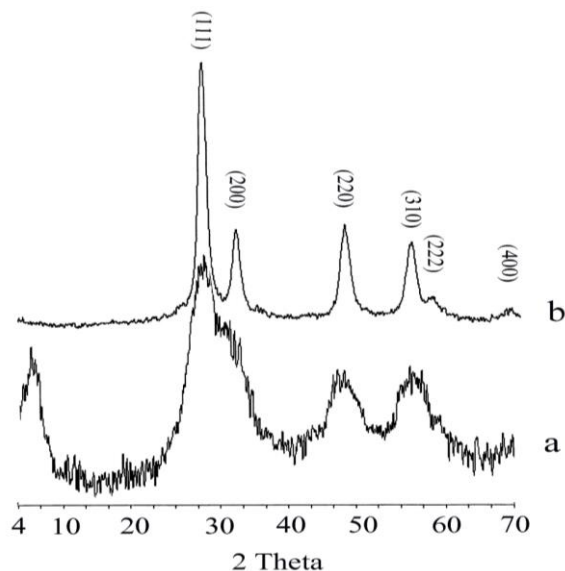


Figure 2: PXRD patterns of a) S₄ and b) S₅.

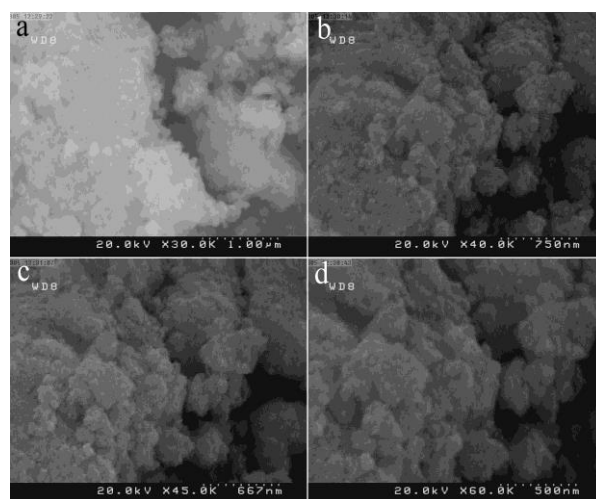


Figure 3: FESEM images of S₁.

Figure 3 shows the FESEM images of S₁. It shows that the obtained materials have particle morphology. Figure 3 a and b show that the material is composed of only particle structure. So the morphology distribution is homogeneous. Figures 3 c and d show that the particle diameter sizes are in the range of about 40-60 nm.

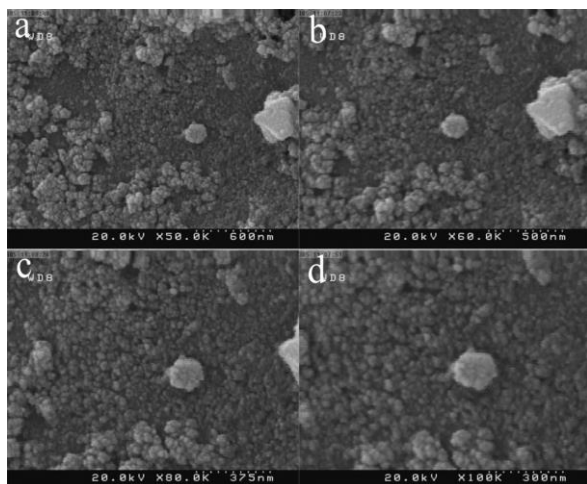


Figure 4: FESEM images of S₂.

Figure 4 shows the FESEM images of S₂. It is clear that the separation of the particles is better than that of S₁. Figures 4 a and b show that the morphology of the synthesized nanomaterials are particles with good size and morphology homogeneity. Figures 4 c and d show that the diameter sizes of the synthesized nanomaterials are about 20 – 40 nm for small particles and 150 – 200 nm for large particles.

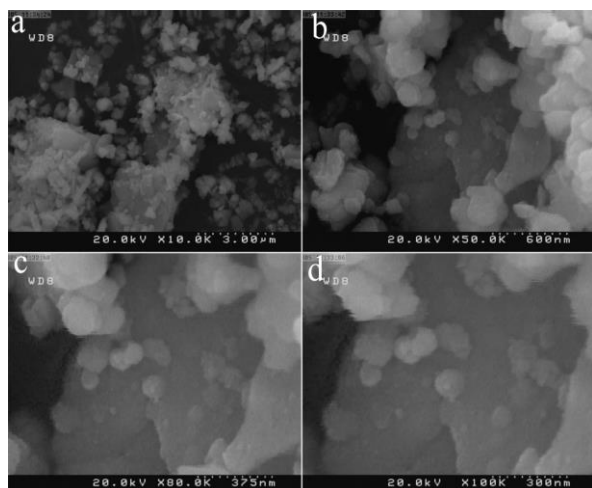


Figure 5: FESEM images of S₃.

Figure 5 shows the FESEM image of S₃. It is clear that the particles morphology is particles without any homogeneity in the size. Figures 5 c and d show that the particles diameter sizes is about 80 - 120 nm. It may be due to using a calcination for the synthesis of S₃ caused the larger particles sized compared to the other samples. It is in

agreement with the interplanar spacing values calculated from PXRD patterns for S₁ and S₃.

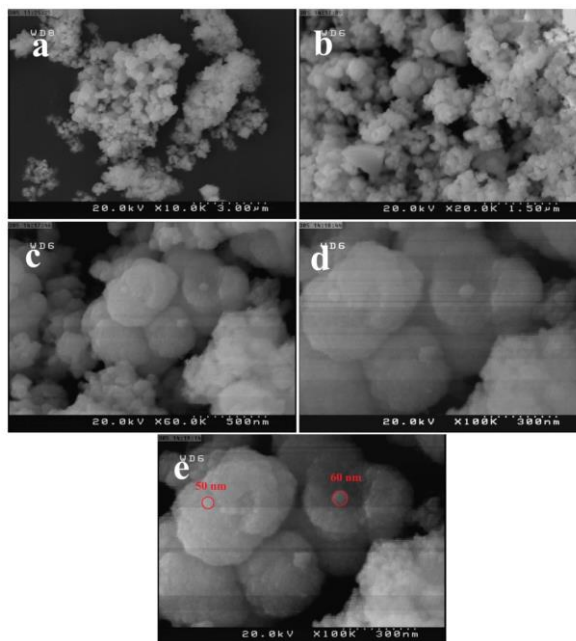


Figure 6: FESEM images of S₄.

Figure 6 shows the FESEM images of S₄. It is clear that with changing the reaction condition and using a low temperature condition for the synthesis of the nanomaterials, the morphology of them were changed. Figures 6 a – d show that the morphology of the synthesized nanomaterials is nearly deficient sphere with small particles as uncus on the surface of it. Figure 6 e shows that the diameter size of the sphere is about 500 – 600 nm and the small particle size of about 50 – 60 nm.

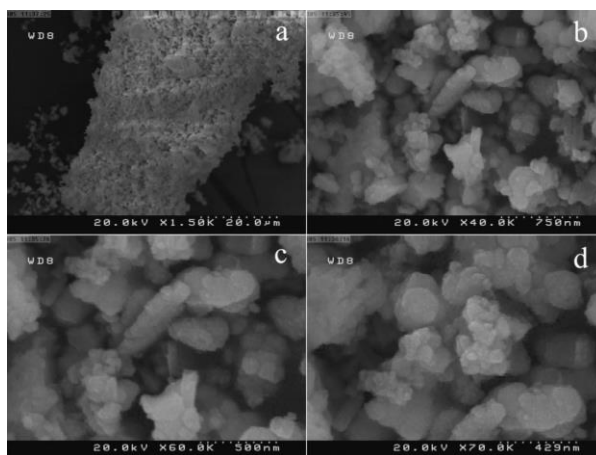


Figure 7: FESEM images of S₅.

Figure 7 shows the FESEM images of S₅. Figures 7 a and b show that obtained material has two kind of flake and particle structures. Figure 7 c shows that the flake thickness size is about 50-70 nm and the length size is about 600 - 650 nm. Figure 7 d shows that the particles diameter sizes are about 40 - 50 nm.

4. Conclusion

Synthesis of CeO₂ nanomaterials in different size and morphology distributions were performed successfully. PXRD data showed that the CeO₂ crystalized in a cubic crystal structure. It showed that the reaction condition is an important parameter in the size and morphology of the synthesized nanomaterials. FESEM images showed that the particles sizes and morphologies were changed with changing the reactions conditions.

Reference

- [1] L. Kepinski, M. Wolcyrz, M. Marchewka, *J. Solid State Chem.* **168** (2002) 110–118.
- [2] A. Trovarelli, M. Boaro, E. Rocchini, C. de Leitenburg, G. Dolcetti, *J. Alloy Compd.* **323** (2001) 584–591.
- [3] T. Tago, S. Tashiro, Y. Hashimoto, K. Wakabayashi, M. Kishida, *J. Nanoparticle Res.* **5** (2003) 55–60.
- [4] G. Wang, Q. Mu, T. Chen, Y. Wang, *J. Alloys Compd.* **493** (2010) 202–207.
- [5] A. S. Araujo, J. C. Diniz, A. O. Da Silva, R. A. Melo, *J. Alloys Compd.* **250** (1997) 532–535.
- [6] J. Xu, G. Li, L. Li, *Mater. Res. Bull.* **43** (2008) 990–995.
- [7] V. Morris, R. Farrell, A. Sexton, M. Morris, *J. Phys. Conf. Ser.* **26** (2006) 119–122.
- [8] S. Sathyamurthy, K. J. Leonard, R.T. Dabestani, M.P. Paranthaman, *Nanotechnology* **16** (2005) 1960–1964.
- [9] A. Gedanken, Ultrason. Sonochem. **11** (2004) 47–55.
- [10] H. Wang, J. J. Zhu, J. M. Zhu, X. H. Liao, S. Xu, T. Ding, H. Y. Chen, *Phys. Chem. Chem. Phys.* **4** (2002) 3794–3799.
- [11] C. Chaisuk, A. Wehatoranawee, S. Preampiyawat, *Ceram. Inter.* **37** (2011) 1459–1463.
- [12] F. Zhang, S.P. Yang, H.M. Chen, X.B. Yu, *Ceram. Inter.* **30** (2004) 997–1002.
- [13] M. Zawadzki, *J. Alloys Compd.* **454** (2008) 347–351.
- [14] A. B. Sifontes, G. Gonzalez, J.L. Ochoa, L.M. Tovar, T. Zoltan, E. Canñizales. *Materials Research Bulletin* **46** (2011) 1794–1799.
- [15] S. d. Carolis, J. L. Pascual, L. G. M. Pettersson, *J. Phys. Chem. B*, **103** (1999) 7627-7636
- [16] A. I. Y. Tok, S. W. Du, F. Y. C. Boey, W. K. Chong, *Materials Science and Engineering A* **466** (2007) 223–229.

